Zhu Jiang (Orcid ID: 0000-0002-0908-5130)
Poulsen Chris (Orcid ID: 0000-0001-5104-4271)

Quantifying the cloud particle-size feedback in an Earth system model

Jiang Zhu[1*] and Christopher J. Poulsen[1]

[1]*Department of Earth and Environmental Sciences, University of Michigan, Ann Arbor, MI 48109*

Geophysical Research Letters

In revision, September 2019

Key Points:

1. Cloud particle size increases with warming in an Earth system model.
2. The associated cloud particle-size feedback is estimated to be 0.18, 0.33 and –0.15 $Wm^{-2}K^{-1}$ for net, shortwave and longwave components.
3. Cloud particle-size feedback is an under-appreciated contributor to the spread of climate sensitivity in current models.

*Corresponding to: Jiang Zhu (jiazhu@umich.edu)

Abstract: Physical process-based two-moment cloud microphysical parameterizations, in which effective cloud particle size evolves prognostically with climate change, have recently been incorporated into global climate models. The impacts of cloud particle-size change on the cloud feedback, however, have never been explicitly quantified. Here we develop a partial radiative perturbation-based method to estimate the cloud feedback associated with particle-size changes in the Community Earth System Model. We find an increase of cloud particle size in the upper troposphere in response to an instantaneous doubling of atmospheric CO_2. The associated net, shortwave and longwave cloud feedbacks are estimated to be 0.18, 0.33 and –0.15 $Wm^{-2}K^{-1}$, respectively. The cloud particle-size feedback is dominated by its shortwave component with a maximum greater than 1.0 $Wm^{-2}K^{-1}$ in the tropics and the Southern Ocean. We suggest that the cloud particle-size feedback is an underappreciated contributor to the spread of cloud feedback and climate sensitivity among current models.

Plain Language Summary: Effects of clouds on Earth's radiation budget vary with their spatial and temporal distribution and their physical properties, including water content and its partitioning between liquid and ice, and cloud particle size. Changes in cloud distribution and physical properties can amplify or damp anthropogenic global warming, and is the largest source of uncertainty in predictions of future climate. The simulation of cloud physical properties in climate models is limited

due to a lack of understanding from theory and observations about what controls these properties. Recent progress has been made in some models to predict cloud particle sizes based on physical processes. In this study, we find an increase of cloud particle size in response to anthropogenic warming and estimate the resulting cloud radiative effects. The larger particles increase scattering of solar radiation in the downward direction leading to an amplification of surface warming. We suggest cloud particle-size changes play a role in the large spread of warming in model predictions of future climate.

1. Introduction

Cloud feedback, the change in top-of-atmosphere radiative flux resulting from the cloud response to warming, ranges in amplitude from weakly negative to strongly positive (–0.13 to +1.24 W m^{-2} K^{-1}) in current climate models and has been identified as the main contributor to the spread of model-based estimates of climate sensitivity (Ceppi, Brient, Zelinka, & Hartmann, 2017). The uncertainty in cloud feedback arises from the complex nature of cloud processes, which occur in multiple cloud regimes and have complicated interactions with various radiative, dynamical and thermodynamic processes including sub-grid scale turbulence and cloud microphysics (see Gettelman and Sherwood (2016) for a review). Decomposing the cloud feedback into contributions from changes in cloud properties provides valuable insights into the physical causes of cloud feedback and its uncertainty in current models (Colman, Fraser, & Rotstayn, 2001; Zelinka, Klein, & Hartmann, 2012). Previous analyses have demonstrated that the cloud feedback is determined by a number of processes including a lifting of free-tropospheric clouds, a decrease of low-cloud amounts at low to middle latitudes and an increase in low-cloud optical depth at middle to high latitudes (Ceppi et al., 2017). Cloud optical depth changes have been further linked to variations in cloud phase and water content (Zelinka et al., 2012).

The role of cloud particle size in the determination of cloud optical properties has long been studied (e.g., Ebert & Curry, 1992; Slingo, 1988; Slingo, 1990; Stephens, 1978), and changes in cloud particle size have been suggested as an important feedback for simulating extreme warm conditions in the past hothouse climate of the Eocene (Kiehl & Shields, 2013; Zhu, Poulsen, & Tierney, 2019). Clouds that contain smaller particles are known to have a larger albedo and smaller infrared emissivity (Liou, 2002). Nonetheless, the processes that control cloud particle size are not well understood, making their incorporation in global climate models a challenge. In most of the early models, particle size was prescribed and invariable (e.g., Kiehl, 1994), precluding a cloud particle-size feedback. In other models, the effective cloud particle size was parameterized as a function of

cloud water content and aerosol number concentration (Martin, Johnson, & Spice, 1994). In recent years, physical process-based two-moment cloud microphysical parameterizations have been developed and implemented into climate models (e.g., Gettelman, Morrison, & Ghan, 2008; Lohmann et al., 2007; Salzmann et al., 2010). These two-moment cloud microphysical schemes increase the degrees of freedom in the system, predicting both cloud water mixing ratio and droplet number concentration. Effective cloud particle size for radiation calculations is diagnosed from cloud water and particle number and allowed to evolve with climate. However, the effects on the cloud feedback from particle-size changes remain to be quantified in climate models with a two-moment cloud microphysical scheme.

In the present study, we develop a method based on the partial radiative perturbation (PRP; Colman et al., 2001; Wetherald & Manabe, 1988; Zhu et al., 2019) to quantify the strength of cloud particle-size feedback in the Community Earth System Model version 1.2 (CESM; Hurrell et al., 2013). The Community Atmosphere Model version 5 (CAM5) in CESM1.2 has a two-moment cloud microphysical scheme that enables the mean cloud particle size to evolve based on physical processes (Gettelman et al., 2008). Our results show an increase of cloud liquid and ice particle size in response to warming caused by an instantaneous doubling of atmospheric CO_2 concentration. The associated shortwave and longwave cloud particle-size feedbacks from PRP calculations are approximately 0.33

and –0.15 W m^{-2} K^{-1}, respectively, resulting in a net feedback of 0.18 W m^{-2} K^{-1}. Given the magnitude of the net feedback, the cloud particle-size feedback seems to be an underappreciated contributor to the spread of cloud feedbacks and climate sensitivity in current models.

2. Model, experiments and method

We employ the CESM1.2 with a horizontal resolution of 1.9 × 2.5° (latitude × longitude) for the atmosphere and land, and a nominal 1° for the sea ice and ocean. The atmosphere model, CAM5, has 30 hybrid sigma-pressure levels. We first conducted two coupled slab ocean model (SOM) simulations: one with a preindustrial CO_2 concentration of 284.7 ppmv and the other with a CO_2 concentration twice that value (hereafter PI and 2xCO2). Other boundary conditions are identical between the two simulations, including the mixed layer depth and heat transport convergence, which were prescribed from a fully coupled preindustrial simulation with dynamic ocean (Bitz et al., 2011). Aerosol emissions were fixed at the preindustrial levels. Our SOM simulations were integrated for 60 years to allow the model to reach equilibrium. We then conducted two parallel atmosphere-only simulations forced with CO_2 concentrations and monthly sea surface temperature and sea-ice cover averaged over the last 30 years from the corresponding coupled SOM simulations. These atmosphere-only simulations were used to generate 10 model years of high frequency fields required for offline radiation calculations. The instantaneous model fields were sampled every 25 model steps (12.5

hours). The sampling length and interval were chosen in consideration of data size, to capture interannual variability, and to provide equal sampling of the zenith angle (Conley, Lamarque, Vitt, Collins, & Kiehl, 2013). All the offline radiation calculations were done using the Parallel Offline Radiative Transfer tool released together with CESM (Conley et al., 2013). The International Satellite Cloud Climatology Project simulator in CAM5 was turned on to allow the application of a radiative kernel method (Kay et al., 2012; Zelinka et al., 2012).

We first calculate the total cloud feedback following the standard "two-way" PRP method (Colman et al., 2001; Wetherald & Manabe, 1988; Zhu et al., 2019). Four offline radiation calculations were carried out to compute the top of the atmosphere (TOA) net radiation flux ($R_{i,j}$). Here, i and j indicate non-cloud (i) and cloud (j) radiation fields taken from either our PI (1) or 2xCO2 (2) experiments, respectively. For example, $R_{1,2}$ denotes the net TOA radiation in the offline calculation driven by fields from the PI experiment but with all cloud-related fields substituted from the 2xCO2 experiment. The net cloud feedback is calculated as

$$\lambda_{cld} = \frac{(R_{1,2}-R_{1,1})+(R_{2,2}-R_{2,1})}{2\Delta T} \quad (1).$$

Here ΔT is the difference in global mean surface temperature between PI and 2xCO2. Note that this method is an average of two substitutions, the cloud-related fields of 2xCO2 into the PI experiment

(1,2) and the PI cloud-related fields into the 2xCO2 experiment (2,1). This "two-way" substitution of cloud fields is performed to remove effects from correlation between cloud and other radiation fields that could contaminant the estimated cloud feedback strength (Colman et al., 2001).

Additional offline radiation calculations were conducted to quantify the feedback from changes in cloud particle size. To illustrate the procedure, we introduce another subscript, k, to our notation of the TOA radiation flux ($R_{i,j(k)}$), which indicates the experiment from which the cloud particle-size field was taken. For example, $R_{1,2(1)}$ denotes the net radiation from offline calculation driven by non-cloud fields from the PI experiment, cloud fields from the 2xCO2 experiment, and cloud particle sizes substituted from the PI experiment. The cloud particle-size feedback can be estimated as

$$\lambda_r = \frac{(R_{1,2(2)}-R_{1,2(1)})+(R_{2,1(2)}-R_{2,1(1)})+(R_{1,1(2)}-R_{1,1(1)})+(R_{2,2(2)}-R_{2,2(1)})}{4\Delta T} \quad (2).$$

Maximum number of possible substitutions are performed here to remove effects from correlation between cloud particle size and other radiation fields.

It is challenging to substitute a single cloud field in one simulation with that from another. For a particular model grid point and time, clouds could exist in one simulation but not the other. Even when there are clouds in both simulations, the cloud characteristics (e.g., stratiform versus convective cloud, cloud water content and phase) could be very different. It is usually inappropriate to simply

swap cloud fields (such as cloud particle sizes), because the radiative effects rely strongly on the combination of the cloud characteristics. To overcome this challenge, we developed a probability density function (PDF)-based approach to substitute cloud particle size between two different simulations. We first divide the globe into small subdomains to avoid substitutions of particle sizes between different cloud regimes. We next calculate for both simulations cloud particle size distribution within the same subdomain at each timestep of the offline radiation calculation. To make a cloud particle-size substitution within a subdomain as in Equation (2), we replace the particle sizes in one simulation with those in the other simulation based on their percentile in the particle size distribution. This statistical approach has the advantage of substituting perfectly the distribution of particle size within a chosen subdomain and preserves the intrinsic relationships between the cloud particle size and the other cloud variables and environmental states. To maintain the three-dimensional large-scale structure of the cloud particle-size distribution (see Figure 1 and related discussion in Section 3) and to ensure enough cloud samples, we have used a subdomain size with a latitude band of ~7.5° and a height of 3 vertical levels. Resampling from a reasonably large subdomain also helps to remove the effect from potential shifts of cloud fields in the latitudinal and vertical direction and obtain the effect from the cloud particle-size changes. The results show a small dependence on subdomain size (<~5%; Table S1). Note that radiation code in CAM5 assumes a gamma distribution of cloud particle size that has intercept and slope parameters. In this case, an

effective particle size is first calculated from the parameters. Intercept and slope parameters are then substituted based on the distribution of the calculated effective particle size. This PDF-based substitution is done for liquid, ice and snow particles separately.

3. Cloud particle-size increase with warming

Figure 1 shows the zonal mean effective cloud particle sizes versus pressure for each simulation. Zonal means were calculated for model grid points with a cloud liquid or ice water mixing ratio greater than 10^{-5}. The largest liquid cloud particles, with radii of ~13 μm, are found in the upper troposphere in the tropics. Secondary maximum centers are located in the troposphere over the subtropics and mid-latitudes in both hemispheres. There exists a north-south asymmetry in liquid cloud particle size with values over the Southern Hemisphere mid-latitudes larger by 1–2 μm than those over the Northern Hemisphere, likely related to the different aerosol concentrations. The effective radius of cloud ice particles in CAM5 ranges approximately from 30 to 90 μm. In the mid- to upper-troposphere, ice particle size varies less with latitude and has maximum values over the tropics. These distributions of cloud particle sizes broadly agree with observations, given the large uncertainty in satellite retrievals of cloud particle sizes (Gettelman et al., 2008; Kay et al., 2012).

Our simulations exhibit an overall increase in the effective radius of cloud liquid and ice particles with warming. In the 2xCO2 experiment, the effective radius of liquid droplets increases by more than 1 μm at higher altitudes (Figures 1b,c). Over the lower latitudes (~30°S–30°N), there is indication of an upward shift of the maximum center of effective radius, as a result of the upward movement of clouds with warming. The secondary maximum centers in liquid droplet size at mid-latitudes show greater values and expand upward and poleward, occupying much more space than in the PI experiment. The effective radius of cloud ice particles increases by ~5 μm, shifting upward with warming in the 2xCO2 experiment. There are changes with mixed signs in ice particle size over the lower troposphere, which, we speculate, have less radiative impact because of the low ice water content and coverage at the lower altitude.

4. A cloud particle-size feedback

The net cloud feedback (λ_{cld}; Equation (1)) from our PRP calculations is 0.60 W m^{-2} K^{-1} with a year-to-year standard deviation of 0.05 W m^{-2} K^{-1} (Table 1). The shortwave and longwave components are 0.46±0.03 and 0.14±0.04 W m^{-2} K^{-1}, respectively. The PRP results agree remarkably well with values using the radiative kernels developed for CAM5 (difference < 0.06 W m^{-2} K^{-1}) (Pendergrass, Conley, & Vitt, 2017). Using a set of radiative kernels from Zelinka et al. (2012), the

difference is as large as 0.24 W m^{-2} K^{-1} for shortwave and longwave components, and serve as a caution against using radiative kernels from different atmospheric models.

The spatial distribution of the net cloud feedback and its shortwave and longwave components are shown in Figures 2 and 3a–c. The net cloud feedback is overall positive with negative values (–0.2—1.2 W m^{-2} K^{-1}) over high latitudes. The net cloud feedback is dominated by its shortwave component over most regions, except for the tropics where there is a strong positive longwave feedback likely associated with the lifting of clouds to higher altitudes (Ceppi et al., 2017). The shortwave cloud feedback is dominated by positive values in stratus and stratocumulus cloud regimes, i.e., the subtropical oceans where there is large-scale subsidence and the storm track regions. These features generally agree with previous studies (Ceppi et al., 2017; Gettelman, Kay, & Shell, 2012; Zelinka et al., 2012).

Our results suggest an important contribution from changes in cloud particle size to the cloud feedback. The PRP calculations show a positive cloud particle-size feedback of 0.18±0.02 W m^{-2} K^{-1}, resulting from a shortwave component of 0.33±0.02 W m^{-2} K^{-1} and an offsetting longwave component of –0.15±0.02 W m^{-2} K^{-1} (Table 1). The net cloud particle-size feedback is nearly one third of the total cloud feedback (0.60 W m^{-2} K^{-1}) in CESM. The shortwave component accounts for approximately 70% of the total shortwave cloud feedback, although there are competing effects from

changes in cloud amount, height and other optical properties (Ceppi et al., 2017; Colman et al., 2001). Similar to the net cloud feedback, the cloud particle-size feedback is dominated by its shortwave component, which is greatest in the tropics and the storm track regions with values reaching 1.0 W m^{-2} K^{-1} (Figure 2). The particle-size feedback in the Southern Hemisphere is greater than in the Northern Hemisphere, consistent with the north-south asymmetric changes in liquid droplet size (Figure 1c). The longwave component of cloud particle-size feedback is negative everywhere and exhibits minimum values of –0.4 W m^{-2} K^{-1} in the tropics. The cloud particle-size feedback has some seasonal variation, moving with the seasonal shift of the Inter-Tropical Convergence Zone (ITCZ) and storm tracks (figure not shown).

The spatial distribution of the cloud particle-size feedback is shown in Figure 3d–f. Over the tropics, the shortwave cloud particle-size feedback resembles the spatial distribution of the ITCZ and has a maximum value of approximately 1.0 W m^{-2} K^{-1}. The shortwave cloud particle-size feedback is 0.2–0.4 and 0.8–1.0 W m^{-2} K^{-1} over the Northern Hemisphere mid-latitude storm track regions and the Southern Ocean high latitudes, respectively. The longwave cloud particle-size feedback is negligible over most of the regions except for the tropics, where a negative feedback reaches –0.6 W m^{-2} K^{-1}. The spatial distribution of the cloud particle-size feedback is consistent with the increase in particle size (Figure 1).

5. Conclusions and discussion

In this study, we find an increase in the effective radius of cloud liquid and ice particles with warming in the Community Earth System Model version 1.2, a model that allows cloud particle size to evolve physically with climate. In response to an instantaneous doubling of atmospheric CO_2, average effective size of liquid cloud particles increases by more than 1 μm in the extratropical and tropical upper troposphere. The average ice particle size also increases with warming by ~5 μm in the upper troposphere. These increases in cloud particle sizes produce more scattering of radiation in the forward direction. The associated radiative effects are quantified using a partial radiative perturbation-based method. It is found that the particle-size changes contribute to a substantial part of the cloud feedback, with a net, shortwave and longwave feedback strength of 0.18, 0.33 and –0.15 W m^{-2} K^{-1}, respectively. The shortwave cloud particle-size feedback is positive everywhere with maxima greater than 1.0 W m^{-2} K^{-1} in the tropics and the Southern Ocean. The longwave cloud particle-size feedback is negative and most significant in the tropics where its magnitude is approximately –0.6 W m^{-2} K^{-1}. Further calculations using CESM suggest a net downward radiative flux at the top of the atmosphere of approximately 1.2 W m^{-2} per μm uniform increase in cloud liquid droplet size (Text S1; Figure S1). We suggest that the net cloud particle-size feedback acts to increase the climate sensitivity in

CESM1.2, as compared to its predecessors in which cloud particle sizes are prescribed and invariant with climate change (Kiehl, 1994).

The cloud particle-size feedback has likely contributed to the large spread in cloud feedback among current models. The cloud particle-size feedback is absent in climate models that prescribe cloud particle size. In models allowing cloud particle size to evolve with climate, the strength of the feedback will depend on the details of the particle-size changes, which, in turn, are closely related to the model physical parameterizations. We emphasize that radiative effects from cloud particle-size changes are intricate and multidimensional, relying on environmental variables and various cloud physical properties, and a comprehensive calculation using three-dimensional general circulations models are required in order to quantify its net contribution to cloud feedback. Further work is needed to investigate the model- and parameterization-dependence of the cloud particle-size feedback. An examination of the newer CESM2 (CAM6) suggests a much larger particle size and greater response to CO_2 forcing than those in CESM1.2 (Figure S2), indicating an important role for cloud particle-size changes to the higher climate sensitivity in CESM2 (Gettelman et al., 2019).

The increase of cloud particle size in CESM1.2 with warming results from the greater rate of increase of in-cloud water content than that of the particle number concentration (Figure S3). The relatively small changes (<20%) in cloud particle number concentration are likely related to the

prescribed preindustrial aerosol emissions in our experiments. These results imply that the positive cloud particle-size feedback identified our experiments acts to compensate the negative cloud feedback from water-content increase; this compensation would be absent if the cloud particle size is prescribed. We note that the cloud particle radii in Figure 1 are from the microphysical scheme of stratiform processes and does not include the contribution from convective clouds. CAM5 assumes that convective clouds have the same particle size as stratiform clouds in the same layer. If stratus clouds do not exist in the same layer, CAM5 specifies an effective radius of ~16.5 μm for liquid droplets, a value that is usually larger than the droplet size from the stratiform scheme (Gettelman et al., 2008; Park, Bretherton, & Rasch, 2014). Therefore, an increased frequency of convective clouds in regions without stratus clouds could be another source for the overall droplet size increases (see Figure S4 for plots of probability density function of droplet size that have accounted for the convective clouds). Although the cloud particle-size feedback in our calculation includes the fast cloud adjustment to CO_2, it is dominated by the SST-mediated change, as the fast adjustment in cloud particle size is negligible (Text S2 and Figure S5). Further observational and theoretical studies are needed to investigate the changes of cloud particle size and number concentration with warming, including the magnitude and spatial pattern, which are critical for better parameterization of cloud particle sizes in global climate models.

Our study identifies a cloud droplet-size feedback that has been underappreciated as a contributor to the total cloud feedback and to the spread of cloud feedbacks and climate sensitivity among current models. Our PRP-based method of diagnosing contributions to the cloud feedback from cloud droplet-size changes has the potential to be extended to quantify cloud feedbacks associated with other cloud properties, which is the goal of our ongoing work.

Acknowledgements: The authors thank X. Huang for helpful discussion. The authors thank the editor and two reviewers for their helpful comments. This work was supported by Heising-Simons Foundation Grant #2016-015 to C. Poulsen. CESM model code is available through the National Center for Atmospheric Research software development repository (https://svn-ccsm-models.cgd.ucar.edu/cesm1/release_tags/cesm1_2_2_1/). Computing and data storage resources, including the Cheyenne supercomputer (doi:10.5065/D6RX99HX), were provided by the Computational and Information Systems Laboratory (CISL) at NCAR. NCAR is sponsored by the National Science Foundation. The authors acknowledge the radiative feedback kernels and related analysis code from A. Pendergrass (https://doi.org/10.5281/zenodo.997899) and M. Zelinka (https://github.com/mzelinka/cloud-radiative-kernels). All relevant data from this study are available

in the Zenodo repository (https://doi.org/10.5281/zenodo.3270654). Additional simulation data can be requested by contacting J.Z. (jiazhu@umich.edu).

References:

Bitz, C. M., Shell, K. M., Gent, P. R., Bailey, D. A., Danabasoglu, G., Armour, K. C., . . . Kiehl, J. T. (2011). Climate Sensitivity of the Community Climate System Model, Version 4. *Journal of Climate, 25*(9), 3053-3070. doi:10.1175/JCLI-D-11-00290.1

Ceppi, P., Brient, F., Zelinka, M. D., & Hartmann, D. L. (2017). Cloud feedback mechanisms and their representation in global climate models. In (Vol. 8, pp. e465-e465): John Wiley & Sons, Inc.

Colman, R., Fraser, J., & Rotstayn, L. (2001). Climate feedbacks in a general circulation model incorporating prognostic clouds. *Climate Dynamics, 18*(1), 103-122. doi:10.1007/s003820100162

Conley, A. J., Lamarque, J. F., Vitt, F., Collins, W. D., & Kiehl, J. (2013). PORT, a CESM tool for the diagnosis of radiative forcing. *Geoscientific Model Development, 6*(2), 469-476. doi:10.5194/gmd-6-469-2013

Ebert, E. E., & Curry, J. A. (1992). A parameterization of ice cloud optical properties for climate models. *Journal of Geophysical Research: Atmospheres, 97*(D4), 3831-3836. doi:10.1029/91jd02472

Gettelman, A., Hannay, C., Bacmeister, J. T., Neale, R. B., Pendergrass, A. G., Danabasoglu, G., . . . Mills, M. J. (2019). High Climate Sensitivity in the Community Earth System Model Version 2 (CESM2). *Geophysical Research Letters, 0*(0). doi:10.1029/2019GL083978

Gettelman, A., Kay, J. E., & Shell, K. M. (2012). The Evolution of Climate Sensitivity and Climate Feedbacks in the Community Atmosphere Model. *Journal of Climate, 25*(5), 1453-1469. doi:10.1175/JCLI-D-11-00197.1

Gettelman, A., Morrison, H., & Ghan, S. J. (2008). A New Two-Moment Bulk Stratiform Cloud Microphysics Scheme in the Community Atmosphere Model, Version 3 (CAM3). Part II: Single-Column and Global Results. *Journal of Climate, 21*(15), 3660-3679. doi:10.1175/2008JCLI2116.1

Gettelman, A., & Sherwood, S. C. (2016). Processes Responsible for Cloud Feedback. *Current Climate Change Reports, 2*(4), 179-189. doi:10.1007/s40641-016-0052-8

Hurrell, J. W., Holland, M. M., Gent, P. R., Ghan, S., Kay, J. E., Kushner, P. J., . . . Marshall, S. (2013). The community earth system model: A framework for collaborative research. *Bulletin of the American Meteorological Society, 94*(9), 1339-1360. doi:10.1175/BAMS-D-12-00121.1

Kay, J. E., Hillman, B. R., Klein, S. A., Zhang, Y., Medeiros, B., Pincus, R., . . . Ackerman, T. P. (2012). Exposing Global Cloud Biases in the Community Atmosphere Model (CAM) Using Satellite Observations and Their Corresponding Instrument Simulators. *Journal of Climate, 25*(15), 5190-5207. doi:10.1175/JCLI-D-11-00469.1

Kiehl, J. T. (1994). Sensitivity of a GCM climate simulation to differences in continental versus maritime cloud drop size. *Journal of Geophysical Research: Atmospheres, 99*(D11), 23107-23115. doi:10.1029/94jd01117

Kiehl, J. T., & Shields, C. A. (2013). Sensitivity of the Palaeocene–Eocene Thermal Maximum climate to cloud properties. *Philosophical Transactions of the Royal Society A: Mathematical, Physical and Engineering Sciences, 371*(2001). doi:10.1098/rsta.2013.0093

Liou, K. N. (2002). *An Introduction to Atmospheric Radiation (Google eBook)* (Vol. 84): Academic Press.

Lohmann, U., Stier, P., Hoose, C., Ferrachat, S., Kloster, S., Roeckner, E., & Zhang, J. (2007). Cloud microphysics and aerosol indirect effects in the global climate model ECHAM5-HAM. *Atmos. Chem. Phys., 7*(13), 3425-3446. doi:10.5194/acp-7-3425-2007

Martin, G. M., Johnson, D. W., & Spice, A. (1994). The Measurement and Parameterization of Effective Radius of Droplets in Warm Stratocumulus Clouds. *Journal of the Atmospheric Sciences, 51*(13), 1823-1842. doi:10.1175/1520-0469(1994)051<1823:Tmapoe>2.0.Co;2

Park, S., Bretherton, C. S., & Rasch, P. J. (2014). Integrating Cloud Processes in the Community Atmosphere Model, Version 5. *Journal of Climate, 27*(18), 6821-6856. doi:10.1175/JCLI-D-14-00087.1

Pendergrass, A. G., Conley, A., & Vitt, F. (2017). Surface and top-of-atmosphere radiative feedback kernels for CESM-CAM5. *Earth System Science Data Discussions*, 1-14. doi:10.5194/essd-2017-108

Salzmann, M., Ming, Y., Golaz, J. C., Ginoux, P. A., Morrison, H., Gettelman, A., . . . Donner, L. J. (2010). Two-moment bulk stratiform cloud microphysics in the GFDL AM3 GCM: description, evaluation, and sensitivity tests. *Atmos. Chem. Phys., 10*(16), 8037-8064. doi:10.5194/acp-10-8037-2010

Slingo, A. (1988). A GCM Parameterization for the Shortwave Radiative Properties of Water Clouds. *Journal of the Atmospheric Sciences, 46*(10), 1419-1427. doi:10.1175/1520-0469(1989)046<1419:AGPFTS>2.0.CO;2

Slingo, A. (1990). Sensitivity of the Earth's radiation budget to changes in low clouds. *Nature, 343*(6253), 49-51. doi:10.1038/343049a0

Stephens, G. L. (1978). Radiation Profiles in Extended Water Clouds. II: Parameterization Schemes. *Journal of the Atmospheric Sciences, 35*(11), 2123-2132. doi:10.1175/1520-0469(1978)035<2123:RPIEWC>2.0.CO;2

Wetherald, R. T., & Manabe, S. (1988). Cloud Feedback Processes in a General Circulation Model. *Journal of the Atmospheric Sciences, 45*(8), 1397-1416. doi:10.1175/1520-0469(1988)045<1397:CFPIAG>2.0.CO;2

Zelinka, M. D., Klein, S. A., & Hartmann, D. L. (2012). Computing and Partitioning Cloud Feedbacks Using Cloud Property Histograms. Part II: Attribution to Changes in Cloud Amount, Altitude, and Optical Depth. *Journal of Climate, 25*(11), 3736-3754. doi:10.1175/jcli-d-11-00249.1

Zhu, J., Poulsen, C. J., & Tierney, J. E. (2019). Simulation of Eocene extreme warmth and high climate sensitivity through cloud feedbacks. *Science Advances, accepted*. doi:10.1126/sciadv.aax1874

Table 1. List of total cloud feedback (λ_{cld}) and the cloud particle-size feedback (λ_r) estimated from partial radiative perturbation method. The feedback is further decomposed into shortwave and longwave components. Total cloud feedback calculated from radiative kernels (the CAM5 kernels from Pendergrass et al. (2017) and the multi-model kernels from Zelinka et al. (2012)) is also listed for comparison. Values in parentheses are the year-to-year standard deviation from 10 years of data. Units are in W m^{-2} K^{-1}.

	λ_{cld}	λ_r	λ_{cld} (Pendergrass kernels)	λ_{cld} (Zelinka kernels)
Net	0.60 (0.05)	0.18 (0.02)	0.62	0.62
SW	0.46 (0.03)	0.33 (0.02)	0.42	0.70
LW	0.14 (0.04)	–0.15 (0.00)	0.20	–0.09

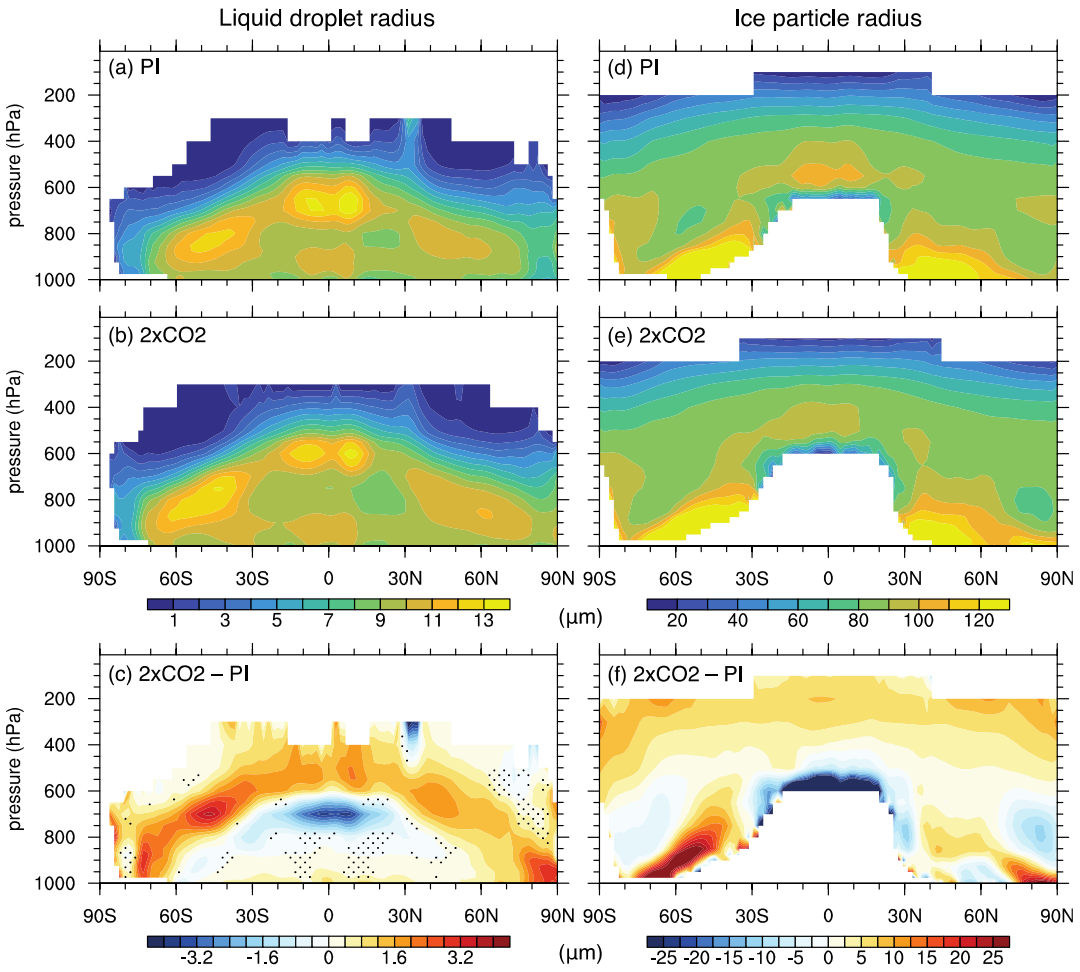

Figure 1. Zonal mean effective radius of cloud liquid droplets versus pressure in the preindustrial **(a)** and the 2xCO2 **(b)** experiments, and the difference between them **(c)**. **(d)**, **(e)** and **(f)** are the same as **(a)**, **(b)** and **(c)**, but for the effective radius of cloud ice particles. Zonal means are constructed for model grid points with cloud liquid/ice water mixing ratio greater than 10^{-5}. Differences in (c) and (f) that are insignificant at the 95% confidence level are stippled. Units are in μm (10^{-6} m). Note that cloud particle radii are from the microphysical scheme of stratiform processes, not including part of the contribution from convective clouds (See Conclusions and discussion**)**.

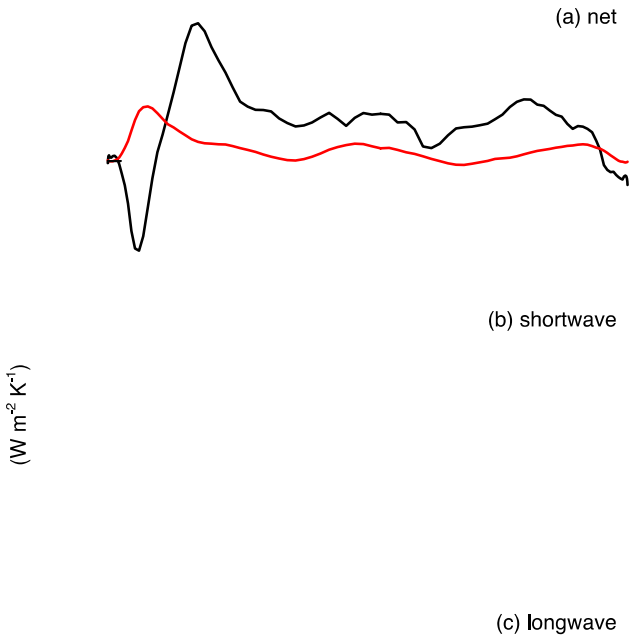

Figure 2. (a) Zonal mean total cloud feedback (black) and the cloud particle-size feedback (red) estimated from the partial radiative perturbation method. **(b)** as in **(a)**, but for the shortwave component. **(c)** as in **(a)**, but for the longwave component. Zonal means are plotted against the sine of latitude. Units are in W m^{-2} K^{-1}. Note that the range on the y-axis differs between subplots.

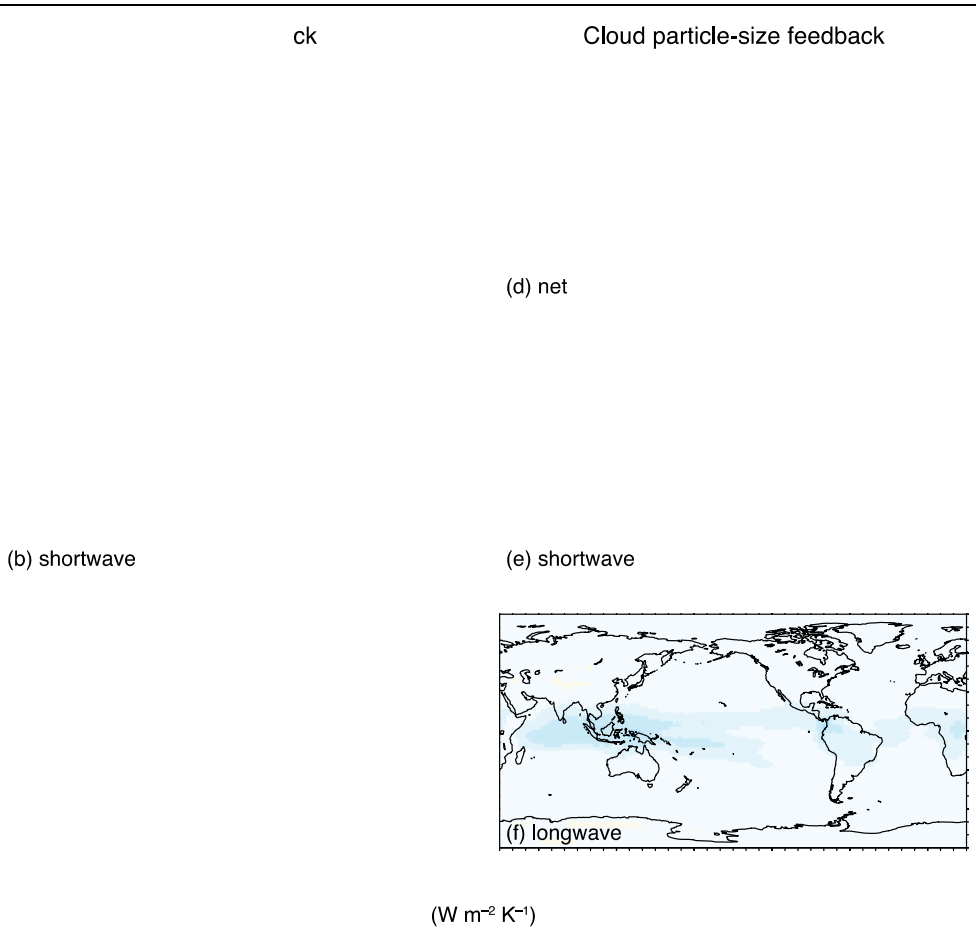

Figure 3. (a) Net cloud feedback estimated from the partial radiative perturbation method and **(b)** its shortwave and **(c)** longwave components. **(d)**, **(e)** and **(f)** as in **(a)**, **(b)** and **(c)**, but for the cloud particle-size feedback. Units are in W m^{-2} K^{-1}.

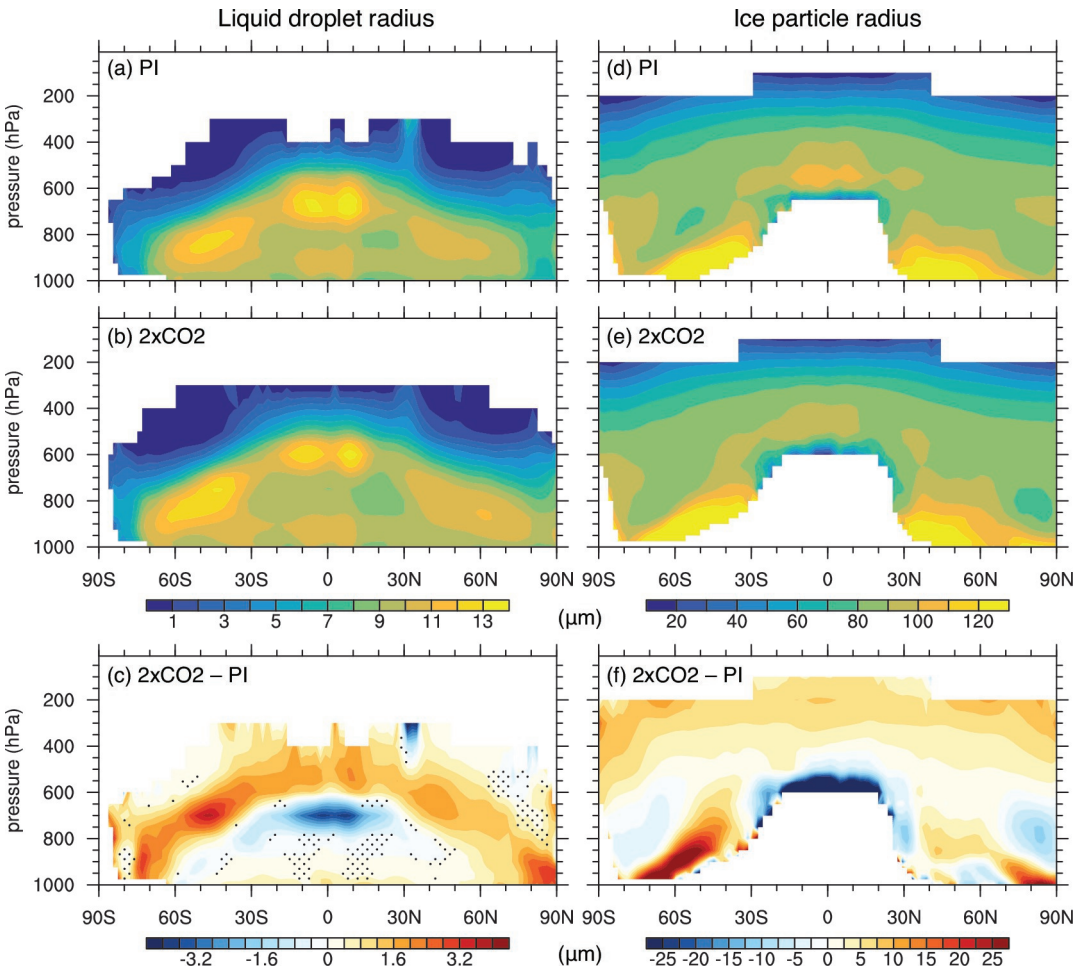

2019gl083829-f01-z-.eps

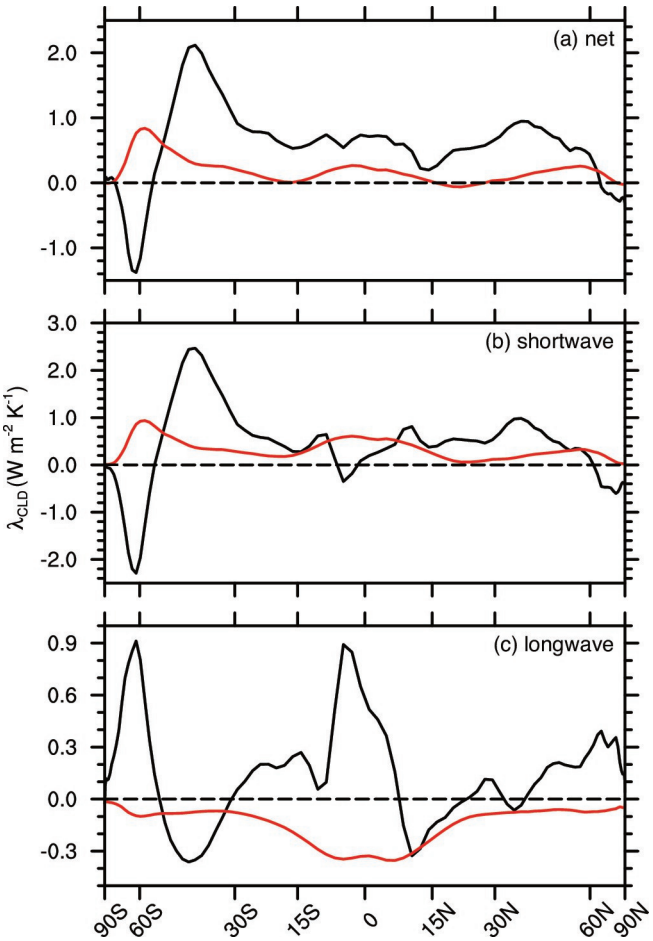

2019gl083829-f02-z-.eps

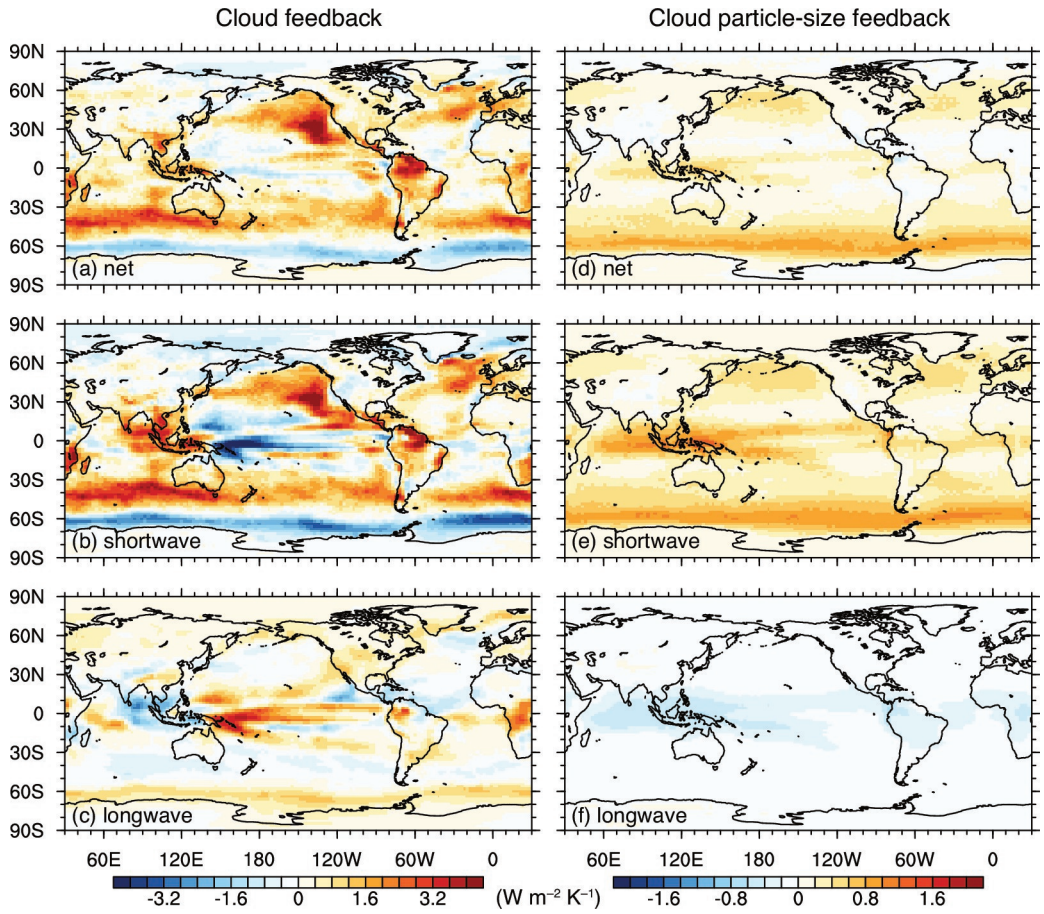

2019gl083829-f03-z-.eps